

Journal of Biomedical Optics

BiomedicalOptics.SPIEDigitalLibrary.org

First biocompatibility margins for optical stimulation at the eardrum via 532-nm laser pulses in a mouse model

Katharina Sorg
Patricia Stahn
Lukas Pillong
Marius P. Hinsberger
Larissa Heimann
Hans-Jochen Foth
Bernhard Schick
Gentiana I. Wenzel

SPIE.

Katharina Sorg, Patricia Stahn, Lukas Pillong, Marius P. Hinsberger, Larissa Heimann, Hans-Jochen Foth, Bernhard Schick, Gentiana I. Wenzel, "First biocompatibility margins for optical stimulation at the eardrum via 532-nm laser pulses in a mouse model," *J. Biomed. Opt.* **24**(8), 085003 (2019), doi: 10.1117/1.JBO.24.8.085003.

First biocompatibility margins for optical stimulation at the eardrum via 532-nm laser pulses in a mouse model

Katharina Sorg,^{a,*} Patricia Stahn,^a Lukas Pillong,^a Marius P. Hinsberger,^a Larissa Heimann,^a Hans-Jochen Foth,^b Bernhard Schick,^a and Gentiana I. Wenzel^{a,*}

^aSaarland University, Department of Otolaryngology, Faculty of Medicine, Homburg, Germany

^bUniversity of Kaiserslautern, Department of Physics, Kaiserslautern, Germany

Abstract. Hearing impairment affects ~460 million people worldwide. Conservative therapies, such as hearing aids, bone conduction systems, and middle ear implants, do not always sufficiently compensate for this deficit. The optical stimulation is currently under investigation as an alternative stimulation strategy for the activation of the hearing system. To assess the biocompatibility margins of this emerging technology, we established a method applicable in whole-mount preparations of murine tympanic membranes (TM). We irradiated the TM of anesthetized mice with 532-nm laser pulses at an average power of 50, 89, 99, and 125 mW at two different locations of the TM and monitored the hearing function with auditory brainstem responses. Laser-power-dependent negative side effects to the TM were observed at power levels exceeding 89 mW. Although we did not find any significant negative effects of optical stimulation on the hearing function in these mice, based on the histology results further studies are necessary for optimization of the used parameters. © The Authors. Published by SPIE under a Creative Commons Attribution 4.0 Unported License. Distribution or reproduction of this work in whole or in part requires full attribution of the original publication, including its DOI. [DOI: [10.1117/1.JBO.24.8.085003](https://doi.org/10.1117/1.JBO.24.8.085003)]

Keywords: biocompatibility; optical stimulation; tympanic membrane; optoacoustic; laser.

Paper 190084RR received Mar. 25, 2019; accepted for publication Jul. 29, 2019; published online Aug. 21, 2019.

1 Introduction

Hearing impairment is a worldwide problem that affects individuals of all ages. There are 460 million people worldwide with hearing impairment and have problems communicating on a daily basis.¹ To compensate for hearing deficit, conventional hearing devices use mechanical energy and, for cases with severe hearing impairment, cochlear implants use electrical energy to stimulate the auditory system. However, for the hard of hearing population who are not yet candidates for cochlear implants and not sufficiently supplied with the currently available auditory prostheses due to multiple reasons, e.g., recurrent outer ear canal inflammations or connectivity issues, further stimulation strategies are needed.² Light has been considered as an alternative energy form for the activation of the hearing organ, having the advantage to be a noninvasive and precise noncontact activation method.^{3–5} The optical stimulation of the ear has been assessed via three different ways, the infrared neural stimulation (INS),^{3,6–9} the optoacoustic stimulation,^{10–12} as well as optogenetics, the activation of neural structures that are genetically modified to express light-sensitive ion channels.^{4,13,14} The optoacoustic stimulation is induced by the use of very short laser pulses that are absorbed into the irradiated materials and lead to a short thermal expansion that induces mechanical vibrations. It was first proposed and studied for the optical stimulation of the inner ear using a monochrome laser.¹⁵ Recently, we were able to demonstrate that the optoacoustic stimulation has the advantage to induce precise vibrations within all vibrating

structures from the ear drum up to the inner ear without the need of direct contact to the vibratory structure.^{2,16,17} Independent of the final irradiated structure, the biocompatibility of this stimulation method has to be defined and characterized. Up to now, just a few specific biocompatibility studies regarding the laser application at the ear drum are to be found in literature. Foth et al. described the power density limits for the laser-induced thermal effects for laser Doppler vibrometry¹⁸ being 7.2 kW/cm² for the pig TM. Another set of studies described the effects of laser irradiation for the low-level laser therapy (LLLT) of the inner ear¹⁹ as well as trans-tympanic photobiomodulation (PBM).²⁰ Both work far below our values using an 830-nm diode laser with power densities of 900 mW/cm² in the case of LLLT and 909 to 1363 mW/cm² for PBM. However, due to the fact that they used another wavelength (830 nm) and that the laser parameters were not exactly in the range of our used parameters, these reports could not give us enough safety margins for a clinical application of the optoacoustic stimulation either. In addition, the tympanic membrane (TM) is anatomically very complex. It consists of collagen fibers, embedded in epithelium with mucosa on the middle-ear side and epidermis on the outside^{21,22} as well as blood vessels. It closes the air-filled tympanic cavity and spans over the bony structure of the malleus. All these together create a very inhomogeneous structure with various absorption characteristics at different locations inducing different laser–tissue interactions. For these reasons, we established a method to assess the biocompatibility margins for light stimulation of the hearing organ and present herein our results regarding the effects of the optoacoustic stimulation with 10-ns 532-nm laser pulses at the TM in a mouse model.

*Address all correspondence to Katharina Sorg, E-mail: Katharina.Sorg@uks.eu; Gentiana I. Wenzel, E-mail: Gentiana.Wenzel@uks.eu

2 Material and Methods

2.1 Animal Model

Eight- to 12-week-old female CBA/J mice (Janvier Labs, France) weighing 18 to 23 g were used in our experiments (44 animals in total in this study). The studies were performed according to the guidelines of “The Animal Care and Use Committee of Saarland.” All animals were initially anesthetized intraperitoneally with 100 mg/kg ketamine (Ketaset, Zoetis, Berlin; Germany), 10 mg/kg xylazine (Rompun, Bayer, Leverkusen; Germany), and a maintenance dose of $\frac{1}{4}$ to $\frac{1}{2}$ of the initial dose intraperitoneally every 30 min. Throughout the experiment, the body temperature of the animal was maintained at 37°C using an electric heating pad, and the animals were supplied with additional oxygen over a tube positioned at nose level. The hearing function of all animals was monitored via auditory brainstem response (ABR) recordings before and within 5 to 10 min after the laser stimulation.

2.2 Surgical Procedure

After we trimmed the hair around the outer auditory canal, we made a vertical incision beginning at the *incisura intertragica* and expanding it along the cartilaginous outer ear canal. The TM was exposed by anchoring the edges of the incision with sutures. To assess possible heat-induced changes by laser irradiation on the TM, a positive control based on heat treatment was established. A 70°C to 80°C preheated metal pin of 0.5 mm diameter was carefully pressed on the TM for 20 s without mechanically damaging the membrane. A further control was the contralateral ear that was left untreated, however that received the same manipulation for the exposure of the TM to ensure the detection of preparation-induced necrotic cell conditions.

2.3 Laser Irradiation

This stimulation protocol was established in cell culture experiments and has been used for the optoacoustic stimulation in the guinea pig in our group as well.² The laser irradiation was always performed on the left ear of the mice. We used a 532-nm pulsed neodymium-doped yttrium orthovanadate (Nd:YVO₄) laser (Xiton Photonics GmbH, Kaiserslautern, Germany) as the light source. The pulsed laser light was applied through a glass fiber with a diameter of 365 μm , which we directed vertically toward the umbo or the *pars tensa* of the TM, at ~ 300 to 500 μm using a micromanipulator (Narishige, Tokyo, Japan). The final adjustments were performed using a continuous wave (cw) pilot laser with a power of 0.1 mW and duration of maximum of 30 s. The laser irradiation parameters were chosen to replicate our self-designed stimulation strategy creating a sinusoid signal at the targeted frequency, the laser-modulation rate (LMR) (Fig. 1).

We irradiated the selected area for 2 min with an average power of either 50, 89, 99, or 125 mW at a laser repetition rate (LPR) of 50 kHz and LMR of 1 kHz as presented in Table 1.

2.4 Electrophysiological Monitoring: Auditory Brainstem Response

The recording of ABRs was performed in the same way as previously reported:^{23–26}

The sounds in the form of sine wave stimuli were generated with a digital signal processing system (Agilent 33500 B Series True form Waveform Generator, Keysight Technologies GmbH,

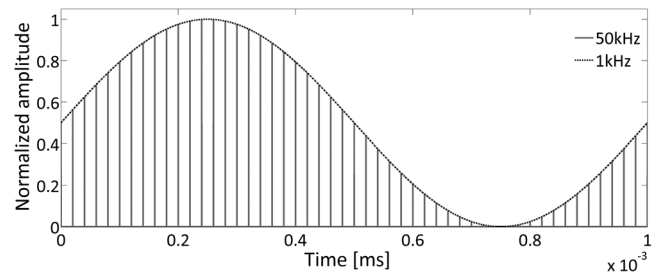


Fig. 1 Our designed stimulation strategy with the laser modulation rate of 1 kHz (black dotted line) and the LPR of 50 kHz (light gray peaks).

Table 1 Used laser parameters.

Average power (mW)	Energy per pulse (μJ)	Average radiant exposure (J/cm^2)	Average power density (W/cm^2)	Irradiation at the umbo (n animals)	Irradiation at the <i>pars tensa</i> (n animals)
50	1	3000	25	7	6
89	1.8	5340	44.5	8	4
99	1.99	5940	49.5	5	5
125	2.5	7500	62.5	4	5

Germany) and were delivered through a free field speaker (custom made from a DT-911, Beyerdynamic GmbH & Co. KG, Germany²⁶) placed in a 5-cm distance in front of the left ear (the irradiated ear). We recorded click- and frequency-specific ABRs using subcutaneous needles: one on the mastoid, one at the vertex (reference), and one at the base of the tail (ground). The recorded signals were then amplified through the biosignal amplifier (g.USBamp, g.tec medical engineering GmbH, Austria), digitized at 19.2 kHz, and filtered to obtain the frequencies from 300 to 2500 Hz. The stimulus intensities ranged from 0 to 80 dB SPL increased in 10 dB steps at 2, 4, 8, 12, 16, 20, 32, and 48 kHz. For click ABRs 500 trials and for fABRs 128 trials were averaged. The speaker output was calibrated periodically. The hearing thresholds were determined visually during the recording as well as offline and were defined by the lowest intensity where the Jewett’s wave complex was identifiable (see Sec. 3, Fig. 5). The Jewett complex was first described by Jewett and Williston in 1971.²⁷ In mice, it typically consists of five vertical positive waves between 1 and 6 ms.^{28–30} We focused on the wave I within the ABR-complex, representing mainly the activity of the first neuron of the auditory pathway³¹ and through this being the closest measure for the function of each ear independently (no crossing neural pathways yet of the auditory pathway). However, due to the small head shadow (diameter of a mouse head being in average 1.2 cm) of mice, one should keep in mind that free field stimulation will always lead to some deterioration and underestimation of ABR measures (see Sec. 4). The amplitude values of wave I were defined by the total value between the first negative peak (I_n) to the first positive peak (I_p) whereas the latency was determined at peak I_p (see Sec. 3, Fig. 4). All animals represented in Table 1 were analyzed ($n = 44$ in total). In a control experiment, ABR measurements were again repeated after 3 h of incubation

($n = 4$ animals). We measured the amplitude of the wave I peak to peak and the latency of the positive part of wave I at the hearing threshold as well as 10, 20, and 30 dB above this.

2.4.1 Fluorescence microscopy

We explanted the petrosal bone of each animal and trimmed down the outer ear canal to its bony part. We then removed the main part of the bony ear canal, down to the bony ring expanding the eardrum as well as parts of the petrosal bone, to expose the TM even better. The tympanic cavity was then opened and trimmed down to the *annulus fibrosus* of the TM. By separating the ossicular chain and cutting the tendon of the *tensor tympani* muscle, the TM was extracted tightly bounded to its bony ring. The explanted TM specimen was placed in 37°C preheated Dulbecco's modified eagle medium and incubated in a 5% CO₂ incubator (Forma Scientific) for 3 h to ensure the maturation of possible cytotoxic effects due to the laser irradiation. After incubation, the specimen was stained for the detection of apoptotic, necrotic, and healthy cells (apoptotic/necrotic/healthy cells detection kit-Promokine; Heidelberg, Germany). This staining protocol was transferred from the cell culture experiments results of our group using the same staining dyes.³² The specimen was washed and subsequently incubated in staining solution, substituted with fluorescence marked Hoechst 33342, Annexin V and Ethidium-Homodimer III for 30 min. After removing the staining solution, the TM specimen was examined

and analyzed under a fluorescence stereomicroscope (Leica Microsystems; Wetzlar, Germany). The three used fluorescent dyes (Fig. 2) mark different cell conditions: healthy cells nuclei were stained only in blue, nuclei of necrotic cells appeared in red and blue, and cells stained with triple colors were dead cells progressing from the apoptotic cell population. The results of the staining were used to quantify the resulting areas of necrotic cells in relation to the whole TM. This was performed with the help of measuring-tools implemented in the microscope software (LASX software, Leica Microsystems, Wetzlar; Germany) and Microsoft Excel[®]. The calculations were performed manually using the measured diameter of the elliptically formed TM and of the necrosis area.

2.4.2 Statistical analysis

The statistical analysis was performed with OriginPro[®] software. If the data were normally distributed and had homogeneity of variance, we conducted two-sided paired *t*-tests for the analysis of the hearing function. Otherwise, the statistical data analysis was performed by Wilcoxon signed-rank test. In case of amplitude and latency measurements, we considered the result of each acoustic stimulation level as an individual value and compared the results before (pre) and after (post) the irradiation at each stimulation level (Figs. 6 and 7). Likewise, we considered each frequency of the fABR analysis as individual values (Fig. 8) and compared the response at each sound level before

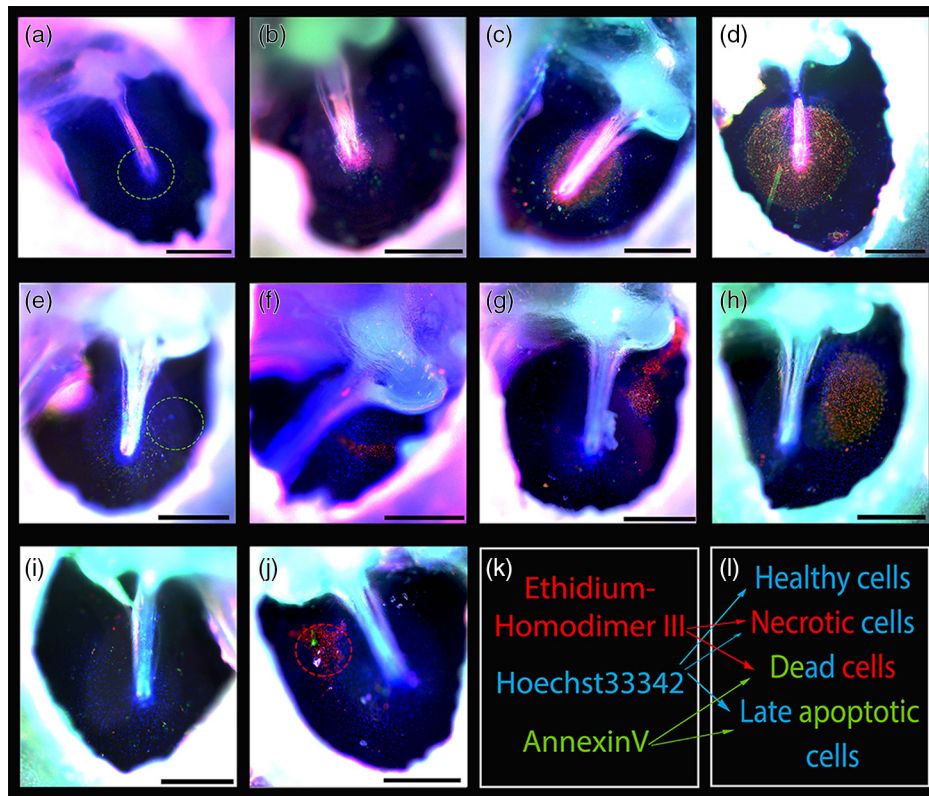


Fig. 2 Fluorescence staining with apoptotic/necrotic/healthy cells detection assay (Promokine, Germany) after irradiation (a)–(d) at the umbo or (e)–(h) at the pars tensa with average power of (a), (e) 50 mW; (b), (f) 89 mW; (c), (g) 99 mW; and (d), (h) 125 mW, respectively. (i) The negative control was not treated; (j) the heat treatment served as a positive control for necrotic cells (red dotted circle). The irradiated region of all specimens is representatively marked as a green dotted circle in the left column. (k) The assay is based on three different stainings which mark specifically (l) different cell conditions. The images demonstrate representative examples of TM. Scale bar represents 500 μm .

and after irradiation. For the control experiment with three measurements, we performed a univariate ANOVA with repeated measures for normally distributed data and otherwise a Friedman-ANOVA. The reported alpha level was 0.05.

3 Results

3.1 Fluorescence Microscopy

We herein present results of the laser application at the umbo and at the *pars tensa* (Figs. 2 and 3). The viability staining performed after laser irradiation gave insight into the distribution of healthy versus apoptotic or necrotic cells within the irradiated TM. The data are presented herein in comparison to the control, nonirradiated ear [Fig. 2(i)] and grouped with respect to the average laser power applied as presented in Table 1. The fluorescence images demonstrate representative examples of the irradiated TM groups.

The results of the fluorescence live/dead staining demonstrated that the laser irradiation with an average power of 50 mW had no effect on the viability of the exposed TM [Fig. 2(a)]. By applying pulses with an average power of 89 mW, first discrete necrotic cell areas around the irradiated location were induced [Figs. 2(b) and 2(f)]. This area of necrotic cells increased in size with increasing laser input (Fig. 3). The irradiations with 99 mW lead to a circular zone of necrotic cells right around the umbo [Fig. 2(c)] and to nearly round areas at the *pars tensa* [Fig. 2(g)]. The necrotic area increased further at 125 mW [Figs. 2(d) and 2(h)]. For the laser application at the *pars tensa*, the thresholds were the same, but the necrotic areas were smaller compared to the irradiation at the umbo. The negative control (nonirradiated TM) [Fig. 2(i)] only demonstrated isolated necrotic or apoptotic cells, which can be attributed to normal physiologic conditions of permanent cell regeneration in the TM. The positive control (heated instrument applied onto the TM) [Fig. 2(j)] leads to an almost round-shaped necrotic cell area similar to the area that was induced through the laser treatment.

The quantification of the proportions of areas with necrotic cells of all irradiated eardrums (see Table 1) confirmed the visually estimated results within the fluorescence imaging (Fig. 3).

The proportion of areas with necrotic cells after the irradiation at the umbo with 89 mW was around $\sim 7\%$ and raised up to $\sim 20\%$ after the irradiation with 125 mW [Fig. 3(a)]. In comparison, the areas with necrotic cells in the *pars tensa* were clearly smaller and grew less in size after the irradiation [Fig. 3(b)]. The proportions were $\sim 1\%$ after the irradiation with 89 mW going to $\sim 6\%$ after the irradiation with 125 mW. The lower increase in necrotic cell areas after irradiation at the *pars tensa* may be due to the fact of a lower absorption of the laser light on the transparent TM compared to the higher absorption at the umbo region, caused by the bony malleus.

3.2 Electrophysiological Monitoring: Auditory Brainstem Response

Figure 4 shows exemplary the filtered ABR signal of one mouse after the stimulation with click acoustic stimuli from 0 to 80 dB SPL. As described in Sec. 2, the threshold was determined as the lowest intensity where the waveform complex I to V was detectable. Typically, the amplitude value at the threshold was around $1 \mu\text{V}$. We also analyzed the averaged hearing thresholds to gain an insight into the effect of laser irradiation. This demonstrated that the mice had an overall hearing threshold at the beginning of the experiment between 10 and 30 dB SPL. We compared the results of the mice irradiated at the umbo [Fig. 5(a)] as well as the ones irradiated at the *pars tensa* [Fig. 5(b)] with the results to the negative control mice (not irradiated) [Fig. 5(c)].

After the irradiation with 50 mW at the umbo, the average threshold increased with 5 dB and after the irradiation with 125 mW around 10 dB. Both increases were, however, statistically not significant. In contrast, no threshold shift could be detected at the other power levels (89 and 99 mW) [Fig. 5(a)]. After the irradiation at the *pars tensa*, the average hearing threshold increase was around 10 dB at all power levels; however, being statistically nonsignificant again [Fig. 5(b)]. In addition, we performed a control experiment in which the animals were anesthetized receiving click ABR and fABR at the same time intervals as in the laser experiments, however without laser exposure [Fig. 5(c)]. In these animals, no threshold shift could be observed. To clarify if there are long-term

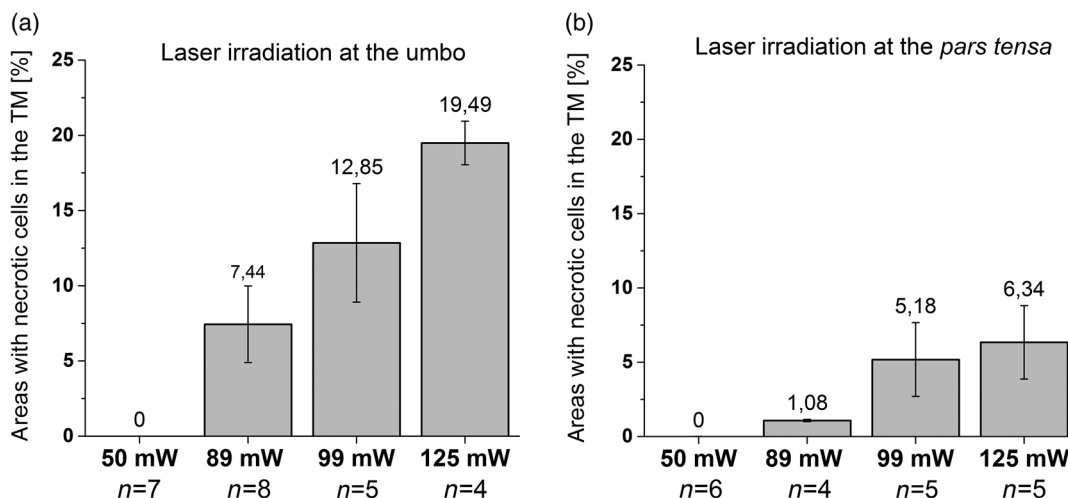


Fig. 3 Proportions of areas with necrotic cells of the whole TM after laser irradiation (a) at the umbo or (b) at the *pars tensa* with 50, 89, 99, and 125 mW, respectively. Error bars represent the SEM. The n indicates the amount of preparations that were analyzed that can also be found in Table 1.

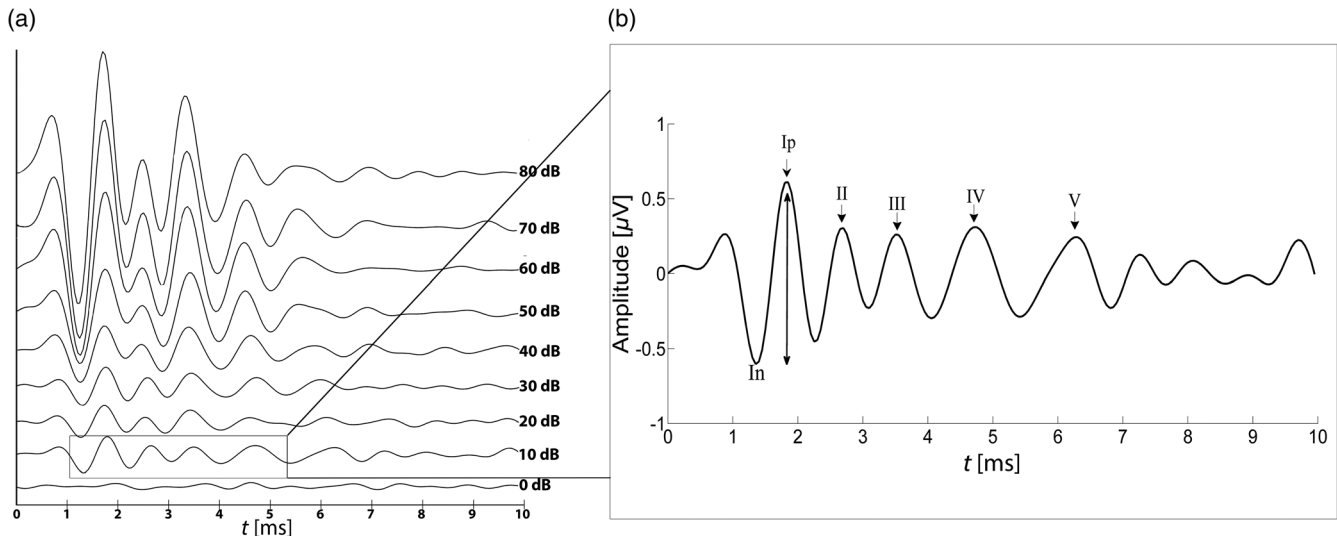


Fig. 4 Example of (a) an evoked click ABR signal from 0 to 80 dB SPL and (b) a filtered detail plot of ABR waves at the threshold (10 dB SPL in this case). At the threshold, the Jewett wave complex consisting of wave I to V is clearly identifiable for the first time above the noise floor. We analyzed wave I in our study and thereby determined the amplitude from peak I_n to I_p and the latency at peak I_p .

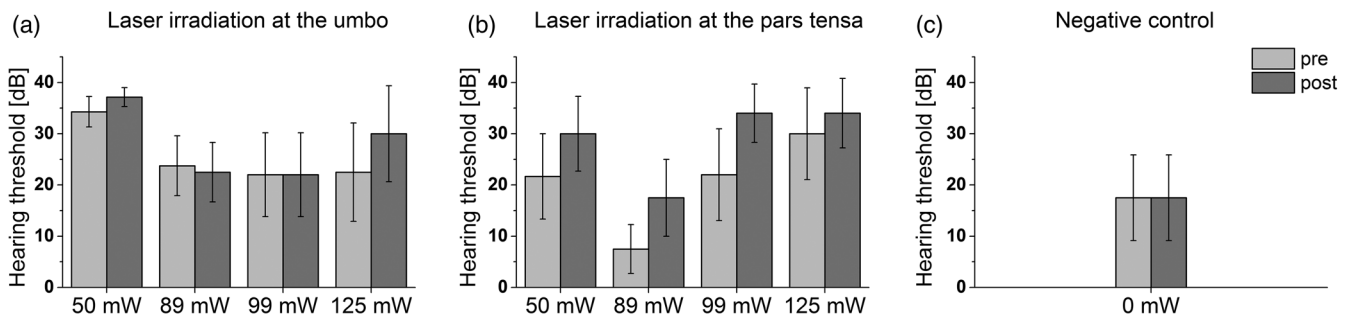


Fig. 5 Click-evoked hearing thresholds of mice that were irradiated (a) at the umbo or (b) at the pars tensa with 50, 89, 99, or 125 mW, respectively. (c) Negative control mice were not irradiated. The error bars represent the SEM.

consequences of these nonstatistically significant differences after laser exposure, further long-term experiments are planned.

In addition to the hearing thresholds, we also analyzed the wave I amplitude and latency values of wave I_p before and after the irradiation as a further measure for the functionality of the auditory pathway (analysis exemplary shown in Fig. 4) at threshold and at 10, 20, and 30 dB above threshold.

The amplitude values demonstrated in all cases the typical increase with higher acoustic stimuli (Fig. 6). For the irradiation at the umbo, the amplitude values started to be nonsignificantly higher after the irradiation with 99 mW having after the irradiation with 125 mW an even more visible increase [Fig. 6(a)]. After the irradiation at the *pars tensa*, the amplitude values were not significantly higher starting from 50 mW [Fig. 6(b)]. At 125-mW irradiation power, the increase between the amplitude of wave I before (pre) and after (post) irradiation was the highest, however lower compared to the irradiation with the same levels at the umbo and being still statistically not significant. In the negative control mice group, we could not detect any differences in amplitude values between before and after the incubation time.

The latency values of the positive peak of wave I (I_p) before and after the irradiation as a measure for the functionality of the

auditory pathway as well as for comparison to the nonirradiated negative control are presented in Fig. 7.

The average latency of wave I varied between 1.6 and 1.8 ms demonstrating a minimal trend to decrease with increasing intensity of the acoustic stimuli [Figs. 7(a) and 7(b)]. The irradiation with 50 mW at the umbo [Fig. 7(a)] induced a significant increase of the latencies at +10 dB over threshold. The irradiation with 99 mW induced a significant increase of the latencies from +0 to +20 dB but being not significant at +30 dB above threshold. The latency values demonstrated a trend to be lower after the irradiation at *pars tensa* [Fig. 7(b)], especially after the irradiation with 99 and 125 mW, this difference being however statistically nonsignificant. One exception could be observed in the negative control mice that demonstrated a significant increase at +30 dB acoustic stimuli. Considering an increased in latency as a negative neural effect, based on these first experiments, no consistent neural damage after the laser irradiation could be detected. The only exception observed was after the irradiation with 99 mW at the umbo that needs to be further explored in future experiments.

Additionally, we analyzed the fABR thresholds of all irradiated and negative-control mice before and after the irradiation, respectively (Fig. 8).

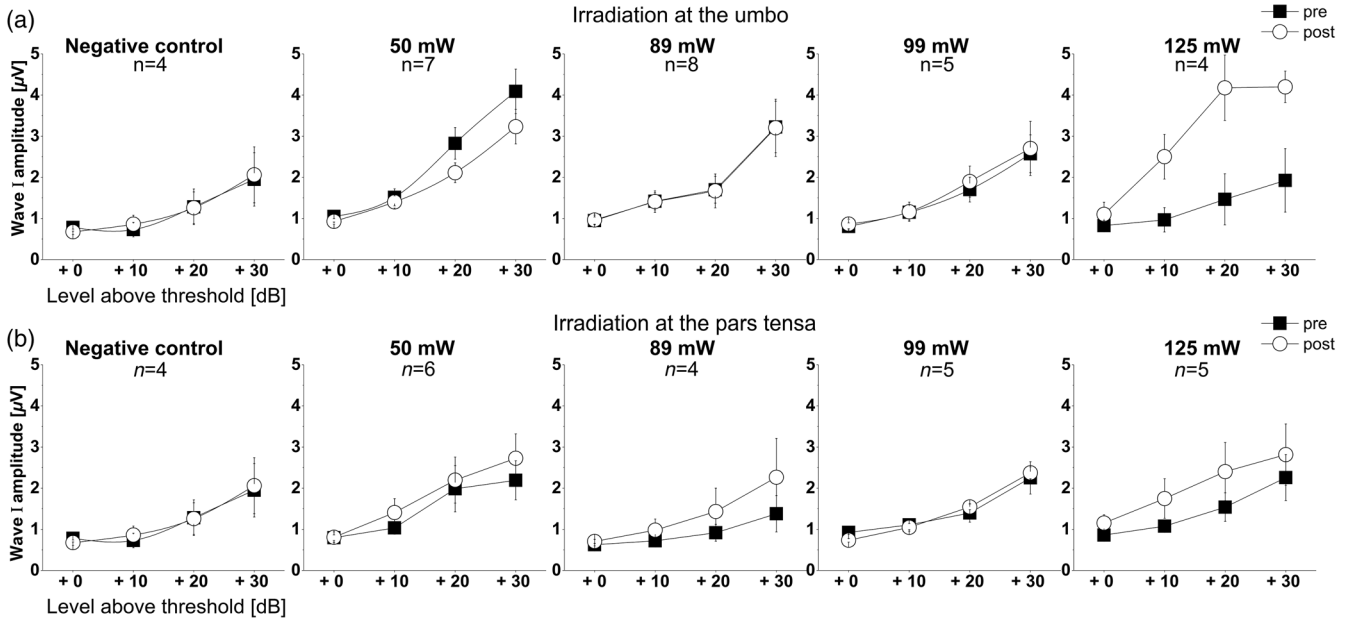


Fig. 6 Analysis of the wave I amplitude before and after the irradiation with 50, 89, 99, and 125 mW average power (a) at the umbo or (b) at the pars tensa. Black squares indicate the amplitude values before (pre) the irradiation, white circles after (post) the irradiation. In both lines, the negative control (nonirradiated mice) experiment is plotted as the reference. Error bars represent the SEM.

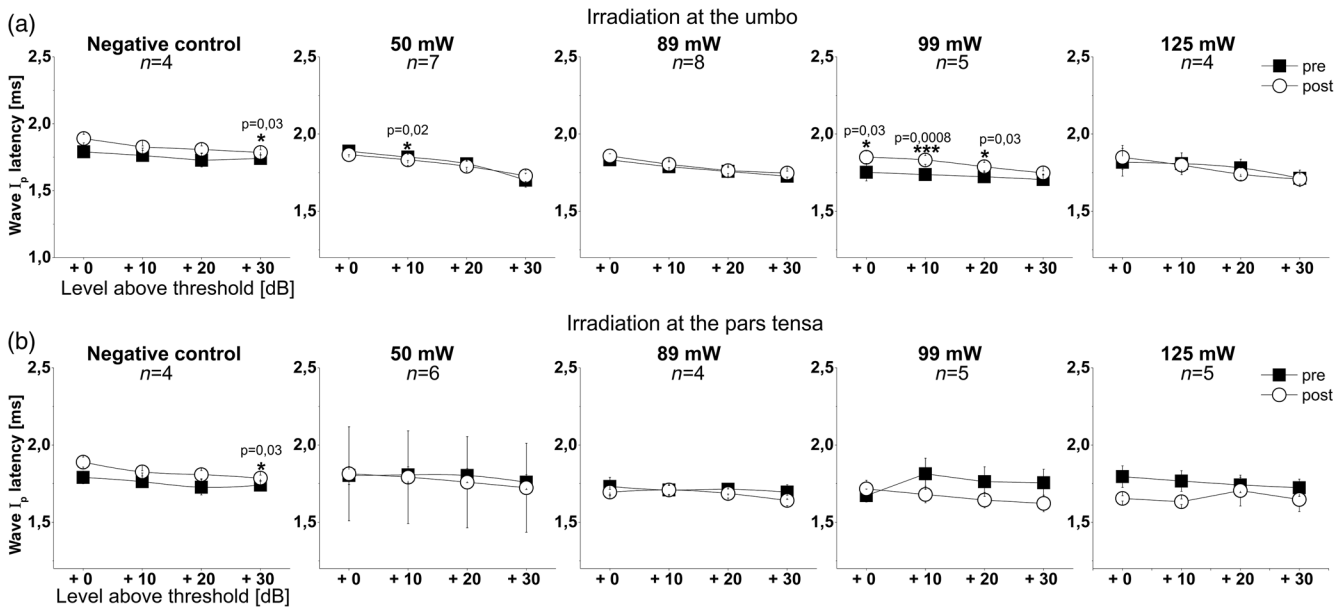


Fig. 7 Analysis of the positive peaks in wave I latency (I_p) before and after the irradiation with 50, 89, 99, and 125 mW average power (a) at the umbo or (b) at the pars tensa. Black squares indicate the latencies before (pre) irradiation, white circles after (post) irradiation. In both lines, the negative control (nonirradiated mice) experiment is plotted as the reference. Error bars represent the SEM and significant different values are marked with a star.

The analysis of the fABR thresholds from 4 to 48 kHz stimulation demonstrated that in all groups the mice had no statistically significant threshold shift with increasing average laser power. The negative control fABRs demonstrated a nonsignificant partial threshold shift as well [Fig. 8(c)]. Interestingly, the threshold shift in these mice after the incubation time was even higher compared to the irradiated mice in the frequencies from 20 up to 48 kHz.

In another control experiment, we analyzed the effects of laser-induced cytotoxicity on the TM on the hearing function within the first 3 h after irradiation on a small collective of animals ($n = 4$). The hearing function was measured before the irradiation with 125 mW at the umbo (pre), directly after the irradiation (post 1) and 3 h later (post 2), analyzing at hearing threshold the wave I amplitude, wave I_p latency and the frequency-specific thresholds (Fig. 9).

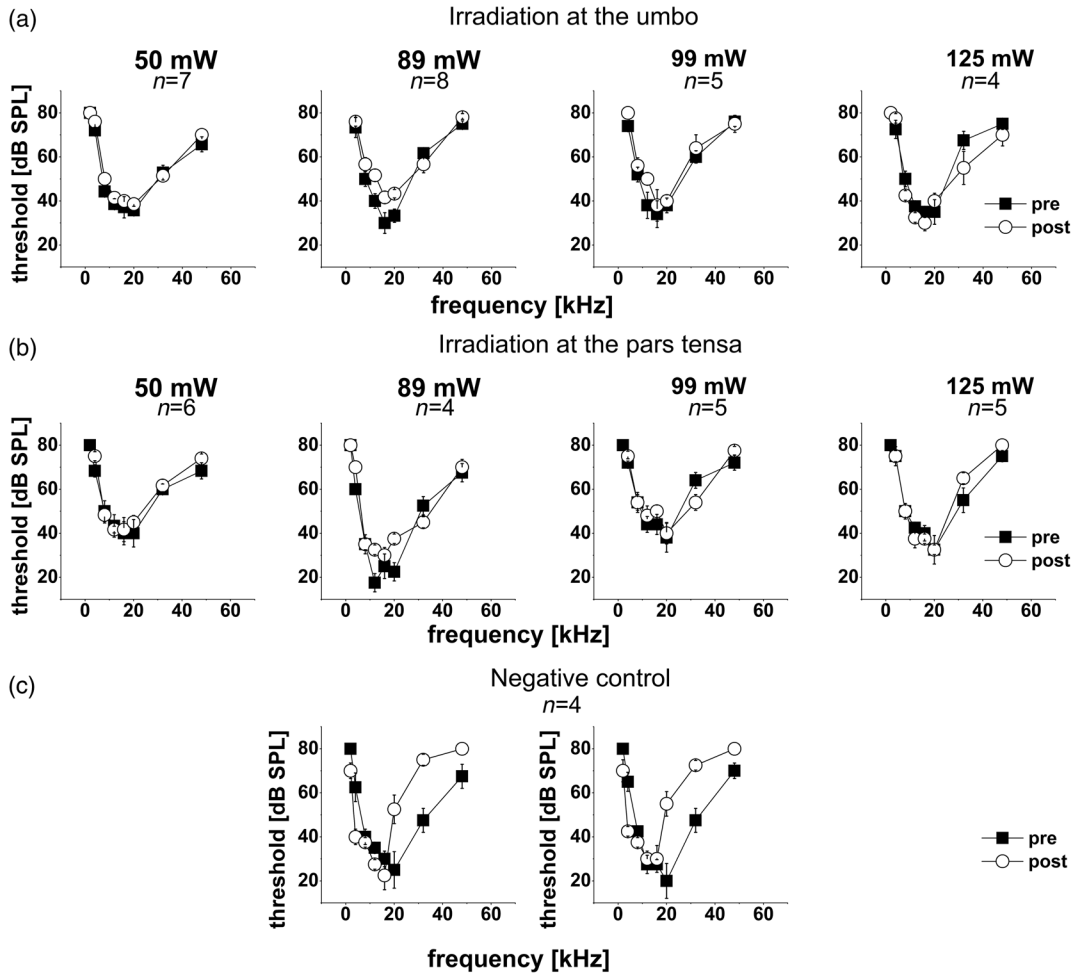


Fig. 8 Analysis of fABR measurements for the irradiation (a) at the umbo and (b) the pars tensa with 50, 89, 99, and 125 mW average laser power, respectively. (a) fABR measurements of the irradiated ear before (pre) and after (post) the irradiation. (b) fABR measurements of the irradiated ear before (pre) and after (post) the irradiation at the pars tensa. (c) Negative control fABR data of the left and the right ear of mice that were not irradiated. Error bars represent the SEM.

Interestingly, the control experiment demonstrated that the average hearing threshold increased with around 10 dB after 3 h of incubation on the irradiated ear being however statistically insignificant in this small group of animals. The fABR analysis showed no significant threshold shift. However, as already mentioned, the nonirradiated contralateral ear could lead to small

deterioration and underestimation of the monaural ABR measurements in this case as well.

4 Discussion

We were able to establish a method for the detection of cytotoxic effects on the TM in a whole-mount model, herein presented to

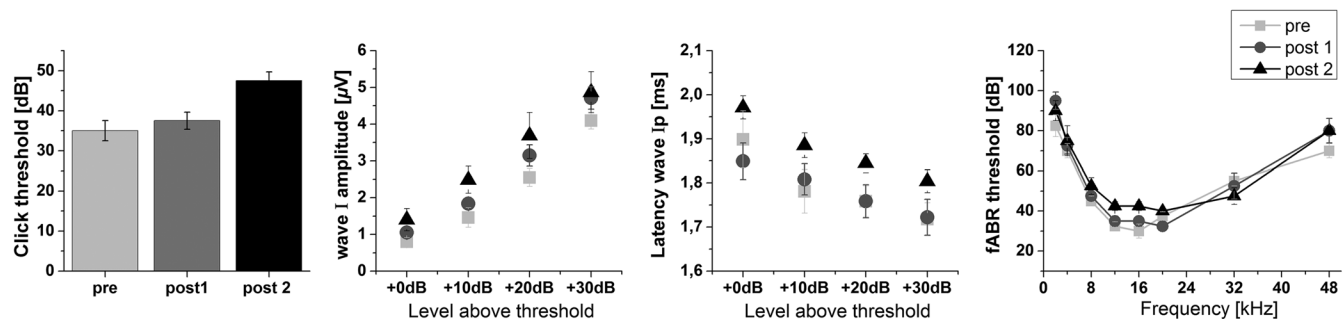


Fig. 9 Analysis of the hearing function of control mice characterized by click ABR threshold, amplitude values of wave I, latency of I_p , and fABR threshold which were measured at three different time points: before the irradiation (pre), directly after (post 1), and 3 h after the irradiation (post 2) $n = 4$.

our knowledge for the first time in the literature. The simultaneous staining of necrotic, apoptotic, and healthy cells gave us insight into the viability of the laser-exposed membrane *in toto*. Additionally, we established a negative and a positive control demonstrating that the staining specifically and repetitively marked necrotic areas within the whole-mount TM mouse model. Using this whole-mount viability assay, we examined the laser-induced effects on the TM after optoacoustic stimulation applied in a sinusoidal form of the pulse sequences. The irradiation with an LPR of 50 kHz and an LMR of 1 kHz for 2 min duration appeared to be safe up to an average power of 50 mW. In our experiments, the irradiation of the eardrum with average laser power of 89 mW induced discrete areas of necrotic cells around the irradiated zone at the umbo as well as at the *pars tensa*. These results could be due to a thermal effect and/or the absorption of green laser light by the surrounding blood vessels in the TM and/or by bony structures, e.g., the umbo or the surrounding tympanic cavity (*bulla tympanica*). Green laser light has been chosen in the originally designed experiments being considered to have a very good biocompatibility potential as visible light. However, our current data demonstrate that through the high absorption of green light by hemoglobin and its clotting effect within the irrigating blood vessels these laser parameters induced cell damage starting at higher laser intensities. In this regard, diminished nutrition and oxygen supply as well as decreased thermal buffering function of the irrigated area are the mechanisms to be discussed. In addition, the affected areas demonstrated to be bigger in the mice irradiated at the umbo compared to those, which received the irradiation at the *pars tensa*. This effect might be caused by at least two factors: (1) the additional high absorption of green laser light within the bony structure of the malleus inducing supplementary heat formation; (2) the clotting effect onto more central vessels in the umbo then at the *pars tensa*. Both may be induced by the fact that the underlying mechanism of the optoacoustic stimulation is a photothermal-laser interaction. In detail, the optoacoustic stimulation is the result of short photon absorption events within the irradiated tissues.^{5,11,16,33,34} The energy introduced by light is converted into kinetic energy, leading to a local increase of the temperature. This rise in temperature will result in a thermoelastic expansion leading at constant volume to an increase in pressure. The permanent alteration between increase and decrease of pressure values during this thermoelastic expansion and relaxation inside of the irradiated material leads to the development of a sound wave that propagates through the irradiated tissue. To gain an optimal stimulation signal, the principle of stress confinement³⁵ should be fulfilled meaning that the laser pulses have to be shorter than the time the acoustic signal needs to propagate through the tissue. Thereby, no energy dissipation happens during the generation of the acoustic signal.¹⁶ However, since we are irradiating inhomogeneous biological structures, the rules of physics cannot be transferred in an absolute mean, and the thermal side effects at high energies can be observed. The safety limits are therefore mandatory to be defined in order to use the optoacoustic effect for stimulation purposes. In our case, one possible reason for the formation of areas with necrotic cells in the TM might be the induction of heat by the high LPR. The thermal damage in laser-tissue interactions in general is dependent on the tissue temperature, the time the tissue remains at the temperature, and the time intervals between the light exposures.³⁶ Computer-based modeling of laser irradiation of the human and the guinea pig cochlea

demonstrated a heat conduction that reached a quasi-steady-state after a few seconds. The rise in temperature was thereby dependent on the laser pulse rate.³⁷ In addition, the photothermal interaction itself is dependent on the diverse properties of the irradiated tissue, e.g., the optical properties (absorption and scattering), the thermal and mechanical properties, the chemical composition as well as the anatomy and the physiology of the irradiated tissue.³⁶ For the TM, these parameters are not sufficiently characterized, yet. Furthermore, the complex histology of the TM consisting of different materials such as bone, collagen fibers, epithelial cells, and blood vessels makes it difficult to investigate the possible laser-tissue interactions just through theoretical calculations. In our case, the absorption of hemoglobin³⁸ and collagen/bone³⁹ appears to play the leading role. Furthermore, the TM as a dry structure, surrounded by air and relatively low-perfused by blood may lead to a low temperature dissipation and therefore to the accumulation of heat during the irradiation period in the TM. Therefore, there is the clear need to define the laser safety parameters and the optical properties of the TM since the laser-tissue interactions are dependent on both: the applied laser parameters and the characteristics of the irradiated structure. As a comparison, in another study in which we chose to use lasers to induce collagen remodeling in the TM, we had to additionally apply a red pigment onto targeted areas of the TM before irradiation to increase its energy absorption and induce the proposed structural changes in our animal model.²³

As briefly mentioned in Sec. 1, very few investigations regarding laser safety for the application at the TM are available in literature. These reports of nondestructive laser application are focusing on the LLLT^{40,41} or PBM.^{20,42} PBM is performed with near-infrared laser light and laser-parameters similar to ours, thus with 165- to 200-mW average power and radiant exposures between 1350 and 3272 J/cm²,^{19,40,43} using macroscopic observation by endoscopy and microscopic observation, e.g., hair cell counting or scanning electron microscopy for assessing the biocompatibility. However, for PBM and LLLT, cw lasers are applied and consequently, the biocompatibility results are hard to compare to the effects of pulsed nanosecond lasers. Another noninvasive application analyzed the thermal thresholds at the TM for laser Doppler vibrometry. This study from Foth et al. presents the safe use of 633-nm cw laser for this application. It reveals a large difference between the power density of 80 W/cm² classically used in laser Doppler vibrometry and the experimental damage threshold of 7100 W/cm² for the irradiation of the pig TM analyzed with via hematoxylin & eosin (H&E).¹⁸ In addition, the studies related to INS,^{3,8,44} e.g., Goyal et al., analyzing the effect of infrared laser light at the cochlea could not find any significant effect within the electrophysiological signals generated in the inner ear after continuous irradiation below 30 μ J/pulse. Histologically, they did not observe any structural changes of the tissue while working with a diode laser at 1869 nm and with 100 μ s pulse length either.⁸

In our study, no significant effects of the irradiation on the hearing function could be demonstrated since any significant increase in hearing thresholds could be detected following the irradiation. The fact that we did not find any correlation between bigger areas with necrotic cells and an increase in hearing threshold after irradiation at the TM is most probably due to the distance from the TM to the sensory cells within the inner ear and therefore too far and insulated by surrounding structures to

be negatively influenced. No significant changes in amplitude values, after the irradiation at the umbo or at the *pars tensa*, could be identified either. This fact conflicted with the finding of higher latency values in one group, after the irradiation at the umbo with 99 mW. Since this effect is singular and has not been confirmed in our experiments in the mice groups irradiated with higher laser intensity, further analyzes need to be performed for a closer characterization of this presumed effect. The results within the negative control mice did demonstrate significantly higher latency values at +30 dB acoustic stimulation, indicating either possible anesthesia-induced effects or physiological changes during the incubation/ irradiation time that need to be taken in account to the cumulative results as well.

The results of the further control experiment analyzing the effects 3 h after the laser exposure did show a nonsignificant trend for higher threshold values. One reason for this might be heat-induced edema formation in the middle ear or the alteration of the vibratory characteristics of the TM. The elasticity of the TM might be influenced by the laser irradiation because of the heat-formation, leading to altered vibrations and thus, changed sound perception to the middle ear and the inner ear. In addition, one should keep in mind the influence of free field stimulation on the contralateral ear and the possible underestimation of the ABR-measurements, which could lead to minor, nonsignificant effects. These possible confounding effects between the ears cannot be easily ruled out in the current presented experimental set. We see the best solution for this in improving our future experimental design regarding this and planning experiments using an animal model that has an increased inter-aural difference.

5 Conclusion

We established a new method to analyze the biocompatibility of light application at the mouse TM. The optoacoustic stimulation at least up to 50 mW was demonstrated to be safe in our experiments. Above 89 mW, the irradiated areas demonstrating cells with affected viability increased with increasing average power. These effects could be due to a thermal effect and/or the absorption of green laser light by the surrounding blood vessels in the TM or by bony structures, such as the umbo or the surrounding *bulla* inducing a debilitating blood supply of the affected tissue. No clear relation between higher laser powers and increased hearing thresholds could be detected in these experiments. Although we did not find any significant negative effect of optoacoustic stimulation on the hearing of mice, we need to improve the used parameters based on the histology results as well as the experimental setup. Further studies are therefore forthcoming for the optimization of the applied laser parameters for a safe optoacoustic stimulation method of the hearing organ.

Disclosures

The authors have no relevant financial interests in this article and no potential conflicts of interest to disclose.

Acknowledgments

This research has been funded by the European Research Council under the European Union's Seventh Framework Program (FP/2007-2013)/ERC Grant, LaserHearingAids: 311469.

References

1. World Health Organization, "Deafness and hearing loss," 2018, <https://www.who.int/news-room/fact-sheets/detail/deafness-and-hearing-loss> (accessed 7 December 2018).
2. P. Stahn et al., "Frequency-specific activation of the peripheral auditory system using optoacoustic laser stimulation," *Sci. Rep.* **9**(1), 4171 (2019).
3. A. D. Izzo et al., "Laser stimulation of the auditory nerve," *Lasers Surg. Med.* **38**(8), 745–753 (2006).
4. T. Moser, "Optogenetic stimulation of the auditory pathway for research and future prosthetics," *Curr. Opin. Neurobiol.* **34**, 29–36 (2015).
5. G. I. Wenzel et al., "Green laser light activates the inner ear," *J. Biomed. Opt.* **14**(4), 044007 (2009).
6. A. D. Izzo et al., "Laser stimulation of auditory neurons: effect of shorter pulse duration and penetration depth," *Biophys. J.* **94**(8), 3159–3166 (2008).
7. H. K. Young et al., "Target structures for cochlear infrared neural stimulation," *Neurophotonics* **2**(2), 025002 (2015).
8. V. Goyal et al., "Acute damage threshold for infrared neural stimulation of the cochlea: functional and histological evaluation," *Anat. Rec.* **295**(11), 1987–1999 (2012).
9. R. U. Verma et al., "Auditory responses to electric and infrared neural stimulation of the rat cochlear nucleus," *Hear. Res.* **310**, 69–75 (2014).
10. G. I. Wenzel, T. Lenarz, and B. Schick, "Welche Farben könnten wir hören?" *HNO* **62**(2), 82–87 (2014).
11. N. Kallweit et al., "Optoacoustic effect is responsible for laser-induced cochlear responses," *Sci. Rep.* **6**(1), 28141 (2016).
12. M. Schultz et al., "Nanosecond laser pulse stimulation of the inner ear: a wavelength study," *Biomed. Opt. Express* **3**(12), 3332–3345 (2012).
13. V. H. Hernandez et al., "Optogenetic stimulation of the auditory nerve," *J. Visual Exp.* (92), e52069 (2014).
14. W. Guo et al., "Hearing the light: neural and perceptual encoding of optogenetic stimulation in the central auditory pathway," *Sci. Rep.* **5**(1), 10319 (2015).
15. A. Fridberger and T. Ren, "Local mechanical stimulation of the hearing organ by laser irradiation," *Neuroreport* **17**(1), 33–37 (2006).
16. K. Zhang et al., "Optoacoustic induced vibrations within the inner ear," *Opt. Express* **17**(25), 23037–23043 (2009).
17. G. I. Wenzel et al., "Effects of green light application at ear drum and middle ear level," in *ARO Midwinter Meeting*, Baltimore (2010).
18. H. J. Foth et al., "Thermal damage threshold at 633 nm of tympanic membrane of pig," *Hear. Res.* **142**(1–2), 71–78 (2000).
19. C.-K. Rhee et al., "Effect of low-level laser treatment on cochlea hair-cell recovery after ototoxic hearing loss," *J. Biomed. Opt.* **18**(12), 128003 (2013).
20. T. H. Moon et al., "Safety assessment of trans-tympanic photobiomodulation," *Lasers Med. Sci.* **31**(2), 323–333 (2016).
21. D. J. Lim, "Human tympanic membrane," *Acta Otolaryngol.* **70**(3), 176–186 (1970).
22. D. J. Lim, "Structure and function of the tympanic membrane: a review," *Acta Otorhinolaryngol. Belg.* **49**(2), 101–115 (1995).
23. S. A. L. Schacht et al., "Laser-induced tissue remodeling within the tympanic membrane," *J. Biomed. Opt.* **23**(12), 121614 (2018).
24. L. Rüttiger et al., "The reduced cochlear output and the failure to adapt the central auditory response causes tinnitus in noise exposed rats," *PLoS One* **8**(3), e57247 (2013).
25. J. Engel et al., "Two classes of outer hair cells along the tonotopic axis of the cochlea," *Neuroscience* **143**(3), 837–849 (2006).
26. T. Schimmang et al., "Lack of Bdnf and TrkB signalling in the postnatal cochlea leads to a spatial reshaping of innervation along the tonotopic axis and hearing loss," *Development* **130**(19), 4741–4750 (2003).
27. D. L. Jewett and J. S. Williston, "Auditory-evoked far fields averaged from the scalp of humans," *Brain* **94**(4), 681–696 (1971).
28. J. J. Chuu, C. J. Hsu, and S. Y. Lin-Shiau, "Abnormal auditory brainstem responses for mice treated with mercurial compounds: involvement of excessive nitric oxide," *Toxicology* **162**(1), 11–22 (2001).
29. K. P. Hunter and J. F. Willott, "Aging and the auditory brainstem response in mice with severe or minimal presbycusis," *Hear. Res.* **30**(2–3), 207–218 (1987).
30. Q. Y. Zheng, K. R. Johnson, and L. C. Erway, "Assessment of hearing in 80 inbred strains of mice by ABR threshold analyses," *Hear. Res.* **130**(1–2), 94–107 (1999).

31. J. F. Willott, "Measurement of the auditory brainstem response (ABR) to study auditory sensitivity in mice," *Curr. Protoc.* **34**(1), 8.21B.1–8.21B.12 (2006).
32. L. Pillong et al., "Biocompatibility studies of optical stimulation via 532 nm-laser pulses on human fibroblasts," *Laryngo-Rhino-Otol.* **97**(S 02), S232 (2018).
33. A. G. Bell, "On the production and reproduction of sound by light," *Am. J. Sci.* **s3-20**(118), 305–324 (1880).
34. M. J. Colles, N. R. Geddes, and E. Mehdizadeh, "The optoacoustic effect," *Contemp. Phys.* **20**(1), 11–36 (1979).
35. G. Paltauf, H. Schmidt-Kloiber, and M. Frenz, "Photoacoustic waves excited in liquids by fiber-transmitted laser pulses," *J. Acoust. Soc. Am.* **104**(2), 890–897 (1998).
36. S. Thomsen, "Pathologic analysis of photothermal and photomechanical effects of laser-tissue interactions," *Photochem. Photobiol.* **53**(6), 825–835 (1991).
37. K. Zhang et al., "A contrastive analysis of laser heating between the human and guinea pig cochlea by numerical simulations," *Biomed. Eng. Online* **15**(1), 59 (2016).
38. B. L. Horecker, "The absorption spectra of hemoglobin and its derivatives in the visible and near infra-red regions," *J. Biol. Chem.* **148**, 173 (1943).
39. J. Behari, S. K. Guha, and P. N. Agarwal, "Absorption spectra of bone," *Calcif. Tissue Res.* **23**(1), 113–114 (1977).
40. Y. M. Park et al., "Trans-canal laser irradiation reduces tinnitus perception of salicylate treated rat," *Neurosci. Lett.* **544**, 131–135 (2013).
41. A. Tamura et al., "Low-level laser therapy for prevention of noise-induced hearing loss in rats," *Neurosci. Lett.* **595**, 81–86 (2015).
42. M. Y. Lee et al., "Photobiomodulation by laser therapy rescued auditory neuropathy induced by ouabain," *Neurosci. Lett.* **633**, 165–173 (2016).
43. C.-K. Rhee et al., "Effect of low-level laser treatment on cochlea hair-cell recovery after acute acoustic trauma," *J. Biomed. Opt.* **17**(6), 068002 (2012).
44. J. D. Wells et al., "Optically mediated nerve stimulation: identification of injury thresholds," *Lasers Surg. Med.* **39**(6), 513–526 (2007).

Katharina Sorg is a PhD student at Saarland University in the Department of Otolaryngology. She received her BS degree in 2013 and her MS degree at University Marburg in biomedical science in 2015. In 2016, she started her PhD. Her current research interests include the effects of optical stimulation on the ear and the development of innovative stimulation strategies for hearing impaired persons, based on the use of light energy.

Biographies of the other authors are not available.